Research Article

Analytical Solutions for Corrosion-Induced Cohesive Concrete Cracking

Hua-Peng Chen[1] and Nan Xiao[1, 2]

[1] *School of Engineering, University of Greenwich, Chatham Maritime, Kent ME4 4TB, UK*
[2] *College of Civil Engineering and Architecture, Zhejiang University, Hangzhou 310058, China*

Correspondence should be addressed to Nan Xiao, sholran@zju.edu.cn

The paper presents a new analytical model to study the evolution of radial cracking around a corroding steel reinforcement bar embedded in concrete. The concrete cover for the corroding rebar is modelled as a thick-walled cylinder subject to axisymmetrical displacement constraint at the internal boundary generated by expansive corrosion products. A bilinear softening curve reflecting realistic concrete property, together with the crack band theory for concrete fracture, is applied to model the residual tensile stress in the cracked concrete. A governing equation for directly solving the crack width in cover concrete is established for the proposed analytical model. Closed-form solutions for crack width are then obtained at various stages during the evolution of cracking in cover concrete. The propagation of crack front with corrosion progress is studied, and the time to cracking on concrete cover surface is predicted. Mechanical parameters of the model including residual tensile strength, reduced tensile stiffness, and radial pressure at the bond interface are investigated during the evolution of cover concrete cracking. Finally, the analytical predictions are examined by comparing with the published experimental data, and mechanical parameters are analysed with the progress of reinforcement corrosion and through the concrete cover.

1. Introduction

The serviceability and durability of concrete structures may be seriously affected by the corrosion of steel reinforcement in structures that are exposed to aggressive environments, such as motorway bridges, car parks, and marine structures. Reinforcement corrosion consumes original steel rebar, generates much lighter rust products, and creates expansive layer at the interface between the reinforcement and the surrounding concrete cover. As corrosion progresses, the expansive displacement at the interface generated by accumulating rust products causes tensile stress in the hoop direction within the concrete cover, leading to radial splitting cracks in the concrete. The cracking and eventually spalling of the concrete

cover significantly affect the bond strength between the rebar and the surrounding concrete cover and consequently influence the service ability and resistance of reinforced concrete structures [1–5]. Therefore, correct predictions of the evolution of cracking in cover concrete and evaluations of residual strength and stiffness of the cracked concrete are of great importance to estimate the remaining life and prevent the premature failure of reinforced concrete structures.

Many investigations have been undertaken during the last two decades regarding the influence of reinforcement corrosion and concrete cracking on the performance of reinforced concrete structures. Al-Sulaimani et al. [6] investigated the influence of reinforcement corrosion on the bond behaviour and strength of reinforced concrete members based on their experimental results. Andrade et al. [7] conducted experiments to monitor the development of crack width on the concrete cover surface induced by the reinforcement corrosion with time. Liu and Weyers [8] presented a model for estimating the time to cracking of concrete cover based on the experiments on various specimen dimensions and corrosion rates. Pantazopoulou and Papoulia [9] proposed a numerical model to study the mechanical implications of cover concrete cracking due to reinforcement corrosion and provided estimates for the time to cover cracking over corroded rebar. Coronelli [10] presented a bond-strength model for predicting the bond strength affected by reinforcement corrosion with reference to rebar position and concrete cover thickness. Recently, Bhargavaa et al. [11] proposed an analytical model for predicting the time required for concrete cover cracking and the weight loss of reinforcement bars due to rebar corrosion. Although considerable research has been conducted on the predictions of the time to concrete cover cracking due to steel rebar corrosion based on the experimental results and the numerical models, limited work has been done on the theory of cracking evolution in cover concrete during the progress of reinforcement corrosion with reference to realistic concrete material properties such as tensile softening behaviour of the cracked concrete and crack band spacing in the concrete cover.

The paper presents a new approach for studying the evolution of cover concrete cracking due to reinforcement corrosion, based on the thick-walled cylinder model for the concrete cover and the cohesive crack model for the cracked concrete. A governing equation for directly solving crack width within cover concrete is established with considering the realistic bilinear softening curve for the cracked concrete and the estimated number of cracks in the concrete cover. The closed-form solutions to crack width are then obtained for various cases that may occur during the evolution of cover concrete cracking. The propagations of the cracked front and critical crack front are investigated, and the time to concrete cover cracking is predicted. Mechanical parameters, such as residual tensile strength, reduced tensile stiffness, and radial pressure at the bond interface, are also studied with the progress of rebar corrosion. Finally, the developed analytical model is examined through its ability to reproduce reported experimental measurements and theoretically provides the evolution of concrete cracking and the deterioration of tensile stiffness and strength of the cracked concrete over the time of reinforcement corrosion.

2. Modelling of Mechanical Problem

The thick-walled cylinder model for concrete cover, initially proposed by Tepfers [12] to analyse the splitting bond strength of reinforcing bars, has been often used for predicting the time for cover concrete cracking due to reinforcement corrosion [8, 9, 11]. A common limitation of most existing analytical models for cover concrete cracking is in
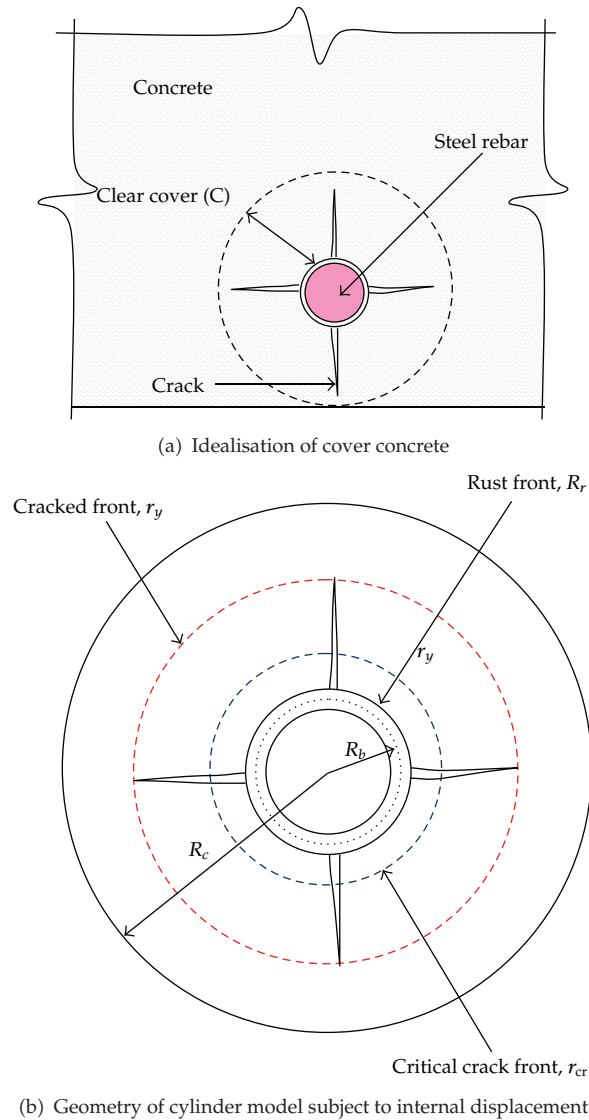
(a) Idealisation of cover concrete

(b) Geometry of cylinder model subject to internal displacement

Figure 1: Thick-walled cylinder model for cover concrete cracking evolution due to reinforcement corrosion.

the representation of the realistic tensile softening behaviour of the cracked concrete, the evolution of cover concrete cracking, and the evaluation of residual tensile strength and stiffness with the progress of reinforcement corrosion.

2.1. Boundary Value Problem for Corrosion-Induced Concrete Cracking

In the thick-walled cylinder model for cover concrete cracking induced by reinforcement corrosion, as shown in Figures 1(a) and 1(b), the reinforcing steel bar has an initial radius R_b embedded in concrete with a clear cover thickness C. The restraint at the internal boundary of the concrete cover could be represented by a prescribed displacement caused by expansive

steel rebar corrosion products. Liu and Weyers [8] reported that a steel rebar may expand by as many as six times its original volume depending on the level of oxidation and estimated the mass of rust products M_r over time t from

$$M_r(t) = \left(4.2 \times 10^{-2}\pi R_b i_{\text{corr}}t\right)^{1/2}, \qquad (2.1)$$

where i_{corr} is mean annual corrosion current per unit length at the surface area of the steel rebar. The increase of volume per unit length due to the rebar corrosion can be obtained from the volume of corrosion rust minus the volume of the original steel rebar consumed, namely,

$$\Delta V = \left(\frac{M_r}{\rho_r} - \frac{M_s}{\rho_s}\right) = \gamma_m M_r, \qquad (2.2)$$

where ρ_s and ρ_r are densities of original steel and corrosion rust, respectively, the mass of original steel consumed M_s is estimated from $M_s = \gamma M_r$ in which coefficient γ is related to the ratio of the mass of rebar consumed over the mass of corrosion rust and could be measured from experiments, and the coefficient γ_m is calculated from $\gamma_m = 1/\rho_r - \gamma/\rho_s$. From the obtained increase of volume, the rust front can be calculated from

$$R_r = \sqrt{R_b^2 + \frac{\Delta V}{\pi}}. \qquad (2.3)$$

To accommodate the volume increase due to steel corrosion, the prescribed displacement at the interface between the steel rebar and the surrounding concrete over time t is given by

$$\bar{u}_b(t) = R_r - R_b = \sqrt{R_b^2 + \frac{\gamma_m}{\pi}M_r(t)} - R_b. \qquad (2.4)$$

The prescribed displacement $\bar{u}_b(t)$ will be considered as the internal boundary condition of the boundary value problem for the evolution of cover concrete cracking. The method described above is based on the general assumption that reinforcement corrosion occurs uniformly and thus the expansion is uniform around the internal boundary of the concrete cover. A recent study by Jang and Oh [13] suggests that in actual aggressive environments reinforcement corrosion may start from the places close to the free surfaces of the concrete cover and thus the rebar may not corrode uniformly in a cross-section. However, the difference in crack development between uniform expansion and nonuniform expansion is small in the case when the corrosion distribution coefficient (i.e., the ratio of the depth of nonuniform corrosion to that of uniform corrosion) does not exceed 2. The uniform corrosion of reinforcement in concrete then could be utilised for the cases with relatively small corrosion distribution coefficients, as shown in many studies such as Bhargavaa et al. [11], Chernin et al. [14], Pantazopoulou and Papoulia [9].

In the case when the prescribed displacement is given, the mass of rust products can be calculated by

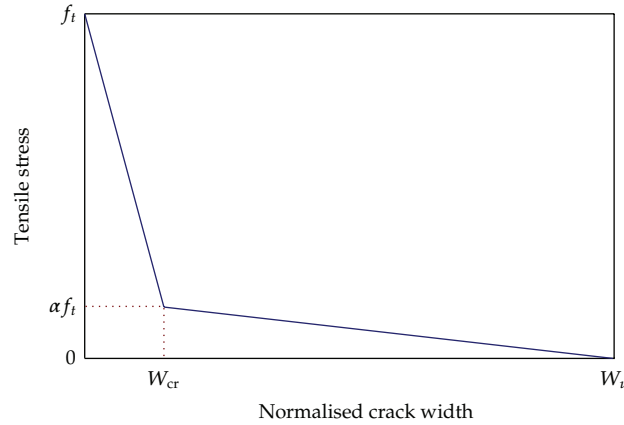$$M_r(t) = \frac{\pi}{\alpha_m}\left[2R_b\bar{u}_b(t) + \bar{u}_b^2(t)\right]. \qquad (2.5)$$

Figure 2: Bilinear softening curve for cohesive cracking in concrete.

Based on the assumption that the steel rebar has uniform corrosion at the surface, the thick-walled cylinder model for cover concrete cracking can be considered as an axis symmetrical problem. The thick-walled cylinder model could be further treated as a plane stress problem because the normal tension-softening stress in the direction of longitudinal axis could be ignored [9], although the approach discussed in this study can also be applied to a plane strain problem. Therefore, the hoop stress in the cylinder is typically a principle tensile stress whereas the radial stress is a principle compressive stress. When the hoop stress reaches the tensile strength of concrete, the radial splitting cracks propagate from the bond interface (R_b) in axis symmetrical directions to the same radius (r_y) until reaching the free surface of concrete cover (R_c), as shown in Figure 1(b). As corrosion progresses the surrounding concrete becomes completely cracked through the cover.

2.2. Cohesive Crack Model for Cracked Concrete

Concrete cracking could be modelled as a process of tensile softening if the cracking is considered as cohesive and the crack width does not exceed a limited value [15, 16]. In cohesive crack model for quasibrittle materials such as concrete, the stress transferred through the cohesive cracks is assumed to be a function of the crack opening [17]. The function (softening curve) can be determined from experiments and may be utilised to replace the stress-strain relations in the theories such as plasticity. Numerous experiments showed that the shapes of various softening curves for different mixes of ordinary concrete are very close to each other. Meanwhile, the bilinear softening curve has been accepted as reasonable approximations of the softening curve for cracked concrete in tension. The bilinear softening curve adopted in the present study is shown in Figure 2 and expressed as

$$\sigma_w = f_t(a - bW), \tag{2.6}$$

where σ_w is the tensile stress crossing cohesive cracks, f_t is the tensile strength of concrete, and W is dimensionless variable that normalises actual crack width $w(r)$ to a nondimensional form and defined as

$$W = \frac{f_t}{G_F} w(r), \tag{2.7}$$

where G_F is the fracture energy of concrete. The coefficients a and b in (2.6) for the bilinear softening curve are given by

$$a = a^{\mathrm{cr}} = 1, \qquad b = b^{\mathrm{cr}} = \frac{(1-\alpha)}{W_{\mathrm{cr}}}, \quad \text{if } 0 \leq W \leq W_{\mathrm{cr}}, \tag{2.8a}$$

$$a = a^{u} = \frac{\alpha W_u}{(W_u - W_{\mathrm{cr}})}, \qquad b = b^{u} = \frac{\alpha}{(W_u - W_{\mathrm{cr}})}, \quad \text{if } W_{\mathrm{cr}} \leq W \leq W_u, \tag{2.8b}$$

where coefficient α, normalised critical crack width W_{cr}, and normalised ultimate cohesive crack width W_u may be determined from experiments. In the CEB-FIB Model Code [18], the coefficient α is given as $\alpha = 0.15$ and W_{cr} and W_u could be evaluated from the maximum aggregate size of concrete materials.

From the crack band theory for the fracture of concrete [19], the total number of cracks n_c separating cracking bands in concrete cover and appearing at cover surface (R_c) may be estimated from

$$n_c = \frac{2\pi R_c}{L_c}, \tag{2.9}$$

where L_c is minimum admissible crack band width estimated from $L_c \approx 3d_a$ in which d_a is maximum aggregate size of concrete. The typical value of total crack number n_c in the thick-walled cylinder model for cover concrete cracking is approximately three or four from the experimental data available [20].

3. Basic Equations

From the results for a thick-walled cylinder subject to internal pressure given by Timoshenko and Goodier [21], the radial stress at a radius follows an inverse square law and diminishes quickly over the radius, approaching zero when the radius is sufficiently large. The effect of the concrete locating at the outside of the thick-walled cylinder shown in Figure 1(a) could be ignored due to the sufficient concrete cover thickness in practice comparing with the diameter of the corroded rebar. The axis symmetrical thick-walled cylinder model with free external surface shown in Figure 1(b), which has been widely utilised in the studies of corrosion-induced concrete cracking such as Bhargavaa et al. [11], Chernin et al. [14], Pantazopoulou and Papoulia [9], can therefore be adopted in this study to represent the surrounding concrete of the corroded bar with a reasonable accuracy. Hence, the boundary value problem of the thick-walled cylinder model for reinforcement corrosion-induced concrete cracking could be considered as an anisotropic nonlinear elastic problem subject to axis symmetrical prescribed displacement at the internal boundary. Based on the cohesive crack model for the radial splitting cracks in the cover concrete, the governing equation associated with crack width for the cracked concrete is derived as follows.

3.1. Equations for Anisotropic Thick-Walled Cylinder

It is well known that, for an anisotropic thick-walled cylinder subject to axis symmetrical actions, radial strain ε_r and hoop strain ε_θ are only related to radial displacement u at radius r, expressed by

$$\varepsilon_r = \frac{du}{dr}, \tag{3.1a}$$

$$\varepsilon_\theta = \frac{u}{r}. \tag{3.1b}$$

For an anisotropic elastic material, the general constitutive relations between radial and hoop stresses (σ_r and σ_θ) and strains are

$$\sigma_r = \frac{1}{1 - \upsilon_{r\theta}\upsilon_{\theta r}}(E_r\varepsilon_r + \upsilon_{r\theta}E_\theta\varepsilon_\theta),$$

$$\sigma_\theta = \frac{1}{1 - \upsilon_{r\theta}\upsilon_{\theta r}}(E_\theta\varepsilon_\theta + \upsilon_{\theta r}E_r\varepsilon_r), \tag{3.2}$$

where E_r is modulus of elasticity in radial direction and E_θ is modulus of elasticity in hoop direction associated with the corresponding crack width of the cracked concrete, $\upsilon_{r\theta}$ and $\upsilon_{\theta r}$ are Poisson's ratios satisfying the requirement of anisotropic elasticity $\upsilon_{\theta r}E_r = \upsilon_{r\theta}E_\theta$.

The stress equilibrium equation for the thick-walled cylinder is

$$\frac{d\sigma_r}{dr} + \frac{1}{r}(\sigma_r - \sigma_\theta) = 0. \tag{3.3}$$

By substituting (3.1a), (3.1b), and (3.2), (3.3) is rewritten as

$$\frac{d^2u}{dr^2} + \frac{1}{r}\frac{du}{dr} - \beta\frac{u}{r^2} = 0, \tag{3.4}$$

where tangential stiffness reduction factor β is introduced to reflect the reduction of the secant tensile stiffness of the cracked concrete in hoop direction during concrete cracking evolution, defined as

$$\beta = \frac{E_\theta}{E_r} = \frac{E_\theta}{E}. \tag{3.5}$$

The stiffness in radial direction E_r is assumed to equal the initial stiffness E of concrete because the radial stress is typically in compression for the boundary value problem

considered. By using the approximation $v = \sqrt{v_{r\theta}v_{\theta r}}$, the stress and strain relations for the boundary value problem given in (3.2) are rewritten as

$$\sigma_r = \frac{E}{1 - v^2}\left(\varepsilon_r + v\sqrt{\beta}\varepsilon_\theta\right), \tag{3.6a}$$

$$\sigma_\theta = \frac{E}{1 - v^2}\left(v\sqrt{\beta}\varepsilon_r + \beta\varepsilon_\theta\right). \tag{3.6b}$$

3.2. Governing Equations for Cracked Concrete

From the cohesive crack model, the residual tensile stress in hoop direction for the cracked concrete can be obtained from

$$\sigma_\theta = \sigma_w = f_t(a - bW). \tag{3.7}$$

The total hoop strain ε_θ of the cracked concrete consists of fracture strain $\varepsilon_\theta{}^f$ and linear elastic strain between cracks $\varepsilon_\theta{}^e$. The fracture strain is generated by a total number of n_c cracks, whereas the linear elastic strain between cracks is associated with the residual tensile hoop stress σ_θ, defined as

$$\varepsilon_\theta{}^f = \frac{n_c w(r)}{2\pi r} = bl_0 \frac{f_t}{E}\frac{W}{r},$$

$$\varepsilon_\theta{}^e = \frac{\sigma_\theta}{E} = \frac{f_t}{E}(a - bW), \tag{3.8}$$

where material coefficient $l_0 = n_c l_{\mathrm{ch}}/2\pi b$ in which l_{ch} is characteristic length $l_{\mathrm{ch}} = EG_F/f_t{}^2$ defined in Hillerborg et al. [17]. The total hoop strain ε_θ of the cracked concrete is then given by

$$\varepsilon_\theta = \varepsilon_\theta{}^f + \varepsilon_\theta{}^e = \frac{f_t}{E}\left[(a - bW) + bl_0\frac{W}{r}\right]. \tag{3.9}$$

The radial displacement u of the cracked concrete, from (3.1b), is calculated from

$$u = \varepsilon_\theta r = \frac{f_t}{E}[(a - bW)r + bl_0 W]. \tag{3.10}$$

And the radial strain, from (3.1a), is given by

$$\varepsilon_r = \frac{f_t}{E}\left[(a - bW) + b(l_0 - r)\frac{dW}{dr}\right]. \tag{3.11}$$

The reduction factor of residual tensile stiffness β defined in (3.5) can be expressed as

$$\beta = \frac{\varepsilon_\theta{}^e}{\varepsilon_\theta{}^e + \varepsilon_\theta{}^f} = \frac{1}{1 + bl_0 W/(a - bW)r}. \tag{3.12}$$

By substituting (3.9) and (3.11), the radial stress in (3.6a) is rewritten as

$$\sigma_r = \frac{f_t}{1 - v^2}\left[\left(1 + v\sqrt{\beta}\right)(a - bW) + b(l_0 - r)\frac{dW}{dr} + v\sqrt{\beta}bl_0\frac{W}{r}\right]. \tag{3.13}$$

The governing equation for directly solving normalised crack width W now can be established by substituting (3.10) and (3.12) into (3.4), expressed here as

$$(l_0 - r)\frac{d^2W}{dr^2} + (l_0 - 3r)\frac{1}{r}\frac{dW}{dr} = 0. \tag{3.14}$$

The general solution to the second-order linear homogeneous differential equation is

$$W = C_1\left[\frac{1}{l_0(l_0 - r)} - \frac{1}{l_0{}^2}\ln\frac{|l_0 - r|}{r}\right] + C_2, \tag{3.15}$$

where constant coefficients C_1 and C_2 in the general solution can be determined from two boundary conditions of the boundary value problem. To calculate radial strains and stresses, the first derivative of the normalised crack width W with respect to radius r is required and given as

$$\frac{dW}{dr} = C_1\frac{1}{r(l_0 - r)^2}. \tag{3.16}$$

To simplify the general solution, a crack width function associated with material coefficient l_0 and radius r within the concrete cover is defined as

$$\delta(l_0, r) = \frac{1}{l_0(l_0 - r)} - \frac{1}{l_0{}^2}\ln\frac{|l_0 - r|}{r}. \tag{3.17}$$

The general solution of normalised crack width given in (3.15) can now be rewritten as

$$W = C_1\delta(l_0, r) + C_2. \tag{3.18}$$

Once the normalised crack width is obtained, mechanical parameters, such as actual crack width, hoop residual strength, and stiffness and radial stress, can be calculated from the corresponding developed equations.

4. Crack Propagation through Cover Concrete

Cracks initiate in cover concrete when the tensile hoop stress at the internal boundary reaches tensile strength and then propagate through the concrete cover until reaching the free cover surface. Depending on the crack width at the internal boundary W_b, three cases are considered at the stage of partially cracked concrete cover, crack initiation at the internal boundary, crack propagation when W_b does not exceed the critical value ($W_b \leq W_{cr}$), and crack propagation when W_b exceeds the critical value ($W_b > W_{cr}$).

4.1. Crack Initiation at Internal Boundary

Since the cover concrete remains intact and elastic before the tensile hoop stress reaches the tensile strength of concrete, the classical elastic solution of radial displacement u to an axis symmetrical thick-walled cylinder [21] is expressed here as

$$u = D_1 r + D_2 \frac{1}{r}, \tag{4.1}$$

where D_1 and D_2 are constant coefficients to be determined by boundary conditions. The radial stress σ_r and hoop stress σ_θ for isotropic elastic materials are given by

$$\sigma_r = \frac{E}{1-v} D_1 - \frac{E}{1+v} D_2 \frac{1}{r^2},$$

$$\sigma_\theta = \frac{E}{1-v} D_1 + \frac{E}{1+v} D_2 \frac{1}{r^2}. \tag{4.2}$$

The displacement boundary condition at the internal boundary (R_b) and the free surface condition at concrete cover surface (R_c) are now introduced:

$$u|_{r=R_b} = \overline{u}_b(t), \qquad \sigma_r|_{r=R_c} = 0, \tag{4.3}$$

where the prescribed displacement $\overline{u}_b(t)$ is given by (2.4). After the constant coefficients D_1 and D_2 are determined from the boundary conditions, the radial and hoop stresses are obtained from

$$\sigma_r = \frac{E R_b}{(1-v)R_b{}^2 + (1+v)R_c{}^2}\left(1 - \frac{R_c{}^2}{r^2}\right)\overline{u}_b, \tag{4.4a}$$

$$\sigma_\theta = \frac{E R_b}{(1-v)R_b{}^2 + (1+v)R_c{}^2}\left(1 + \frac{R_c{}^2}{r^2}\right)\overline{u}_b. \tag{4.4b}$$

It can be seen that the hoop stress is in tension whereas the radial stress is in compression over the concrete cover. The cover concrete initiates cracking when the hoop stress σ_θ at

the internal boundary reaches the tensile strength f_t. From (4.4b), the radial displacement at the internal boundary at the time to crack initiation T_i can be calculated from

$$\overline{u}_b(T_i) = \frac{(1-v)R_b{}^2 + (1+v)R_c{}^2}{R_b{}^2 + R_c{}^2} \frac{f_t}{E} R_b. \tag{4.5}$$

The corresponding mass of corrosion rust at the time to crack initiation is obtained from (2.5), and then the time when cracking initiates at the internal boundary (T_i) can be estimated from (2.1).

4.2. Crack Propagation before Crack Width at Rebar Surface Reaches Critical Value

The thick-walled cylinder is now divided into two zones, an intact outer ring ($r_y{}^+ \leq r \leq R_c$) and a cracked inner ring ($R_b \leq r \leq r_y{}^-$). In the intact outer ring, the tensile hoop stress reaches the concrete tensile strength f_t at the crack front ($r_y{}^+$) and the external surface (R_c) remains free, expressed as

$$\sigma_\theta|_{r=r_y{}^+} = f_t, \qquad \sigma_r|_{r=R_c} = 0. \tag{4.6}$$

From (4.2) and by using the constant coefficients D_1 and D_2 determined from the boundary conditions, the radial and hoop stresses are given by

$$\sigma_r = \frac{f_t r_y{}^2}{r_y{}^2 + R_c{}^2}\left(1 - \frac{R_c{}^2}{r^2}\right), \tag{4.7a}$$

$$\sigma_\theta = \frac{f_t r_y{}^2}{r_y{}^2 + R_c{}^2}\left(1 + \frac{R_c{}^2}{r^2}\right). \tag{4.7b}$$

In the cracked inner ring, where the crack width at the internal boundary does not exceed the critical value, the displacement condition at internal boundary (R_b) described in (4.3), by using (3.10) and considering (2.8a), is rewritten as the boundary condition for the normalised crack width

$$W_b{}^{\mathrm{cr}}(t) = \frac{1}{b^{\mathrm{cr}}\left(l_0{}^{\mathrm{cr}} - R_b\right)}\left(\frac{E}{f_t}\overline{u}_b(t) - a^{\mathrm{cr}}R_b\right), \tag{4.8}$$

where material coefficient $l_0{}^{\mathrm{cr}} = n_c l_{\mathrm{ch}}/2\pi b^{\mathrm{cr}}$. Meanwhile, considering zero crack width at the crack front ($r_y{}^-$), the boundary conditions for the cracked zone are expressed as

$$W|_{r=R_b} = W_b{}^{\mathrm{cr}}, \qquad W|_{r=r_y{}^-} = 0. \tag{4.9}$$

From (3.18) and by using the boundary conditions, the normalised crack width over the cracked inner ring is given by

$$
W = \frac{\delta(l_0{}^{\mathrm{cr}}, r) - \delta(l_0{}^{\mathrm{cr}}, r_y)}{\delta(l_0{}^{\mathrm{cr}}, R_b) - \delta(l_0{}^{\mathrm{cr}}, r_y)} W_b{}^{\mathrm{cr}}. \tag{4.10}
$$

The crack front (r_y) can be determined by the continuity condition of radial stress crossing the intact and cracked zones, namely,

$$
\sigma_r|_{r=r_y{}^+} = \sigma_r|_{r=r_y{}^-}. \tag{4.11}
$$

From (4.7a), the radial stress at the internal boundary of the intact zone $(r_y{}^+)$ is given by

$$
\sigma_r|_{r=r_y{}^+} = \frac{r_y{}^2 - R_c{}^2}{r_y{}^2 + R_c{}^2} f_t. \tag{4.12}
$$

By using (4.10) and considering $\beta = 1$ at the crack front, the radial stress at the external boundary of the cracked zone $(r_y{}^-)$, from (3.13), is given by

$$
\sigma_r|_{r=r_y{}^-} = \frac{f_t}{1 - v^2} \left[(1 + v) - \frac{(1 - \alpha)}{r_y(l_0{}^{\mathrm{cr}} - r_y)[\delta(l_0{}^{\mathrm{cr}}, r_y) - \delta(l_0{}^{\mathrm{cr}}, R_b)]} \frac{W_b{}^{\mathrm{cr}}}{W_{\mathrm{cr}}} \right]. \tag{4.13}
$$

The boundary condition in (4.11) for determining the crack front (r_y) gives

$$
r_y(l_0{}^{\mathrm{cr}} - r_y)[\delta(l_0{}^{\mathrm{cr}}, r_y) - \delta(l_0{}^{\mathrm{cr}}, R_b)] \left[(1 + v) + \left(1 - v^2\right) \frac{R_c{}^2 - r_y{}^2}{R_c{}^2 + r_y{}^2} \right] = (1 - \alpha) \frac{W_b{}^{\mathrm{cr}}}{W_{\mathrm{cr}}}. \tag{4.14}
$$

When the crack front reaches the concrete cover surface $(r_y = R_c)$, the normalised crack width at the internal boundary at the time to cracking on cover surface (T_c) is calculated from

$$
W_b{}^{\mathrm{cr}}(T_c) = (1 + v) R_c (l_0{}^{\mathrm{cr}} - R_c)[\delta(l_0{}^{\mathrm{cr}}, R_c) - \delta(l_0{}^{\mathrm{cr}}, R_b)] \frac{W_{\mathrm{cr}}}{1 - \alpha}. \tag{4.15}
$$

From (4.8), the corresponding displacement at the internal boundary of the thick-walled cylinder at time T_c can be determined from

$$
\overline{u}_b(T_c) = \left\{ 1 + (1 + v) \frac{R_c}{R_b} (l_0{}^{\mathrm{cr}} - R_b)(l_0{}^{\mathrm{cr}} - R_c)[\delta(l_0{}^{\mathrm{cr}}, R_c) - \delta(l_0{}^{\mathrm{cr}}, R_b)] \right\} \frac{f_t}{E} R_b. \tag{4.16}
$$

Consequently, the time to cracking T_c can be estimated from (2.5) and (2.1). It can be seen that the time to cracking is a function of concrete cover dimensions, material properties of cover concrete, and reinforcement corrosion rate.

4.3. Crack Propagation When Crack Width at Rebar Surface Exceeds Critical Value

In this case, the thick-walled cylinder is divided into three zones, as shown in Figure 1(b), an intact outer ring ($r_y^+ \leq r \leq R_c$), a cracked middle ring, where crack width does not exceed critical value ($r_{cr}^+ \leq r \leq r_y^-$), and a cracked inner ring, where crack width exceeds critical value ($R_b \leq r \leq r_{cr}^-$). The intact outer ring of this case has the same results given in Section 4.2. For the cracked middle ring, considering the critical crack width at the internal boundary (r_{cr}^+), the boundary conditions for the cracked middle ring are

$$W|_{r=r_{cr}^+} = W_{cr}, \qquad W|_{r=r_y^-} = 0. \tag{4.17}$$

The normalised crack width within the cracked middle ring is then given by

$$W = \frac{\delta(l_0^{cr}, r) - \delta(l_0^{cr}, r_y)}{\delta(l_0^{cr}, r_{cr}) - \delta(l_0^{cr}, r_y)} W_{cr}. \tag{4.18}$$

For the cracked inner ring, because the crack width exceeds the critical value, from (3.10) and (2.8b), the normalised crack width at its internal boundary is given by

$$W_b^u(t) = \frac{1}{b^u(l_0^u - R_b)} \left(\frac{E}{f_t} \overline{u}_b(t) - a^u R_b \right), \tag{4.19}$$

where material coefficient $l_0^u = n_c l_{ch}/2\pi b^u$. The boundary conditions for the cracked inner ring are

$$W|_{r=R_b} = W_b^u, \qquad W|_{r=r_{cr}^-} = W_{cr}. \tag{4.20}$$

Therefore, the normalised crack width within the cracked inner ring is given by

$$W = \frac{\delta(l_0^u, r) - \delta(l_0^u, r_{cr})}{\delta(l_0^u, R_b) - \delta(l_0^u, r_{cr})} W_b^u + \frac{\delta(l_0^u, R_b) - \delta(l_0^u, r)}{\delta(l_0^u, R_b) - \delta(l_0^u, r_{cr})} W_{cr}. \tag{4.21}$$

Considering the condition of radial stress continuity at the crack front (r_y) between the intact ring and the cracked middle ring described in (4.11), an equation similar to (4.14) is obtained

$$r_y(l_0^{cr} - r_y) \left[\delta(l_0^{cr}, r_y) - \delta(l_0^{cr}, r_{cr}) \right] \left[(1 + v) + \left(1 - v^2 \right) \frac{R_c^2 - r_y^2}{R_c^2 + r_y^2} \right] = 1 - \alpha. \tag{4.22}$$

Meanwhile, the condition of radial stress continuity at the critical crack boundary (r_{cr}) between the cracked middle ring and the cracked inner ring gives

$$\sigma_r|_{r=r_{cr}^+} = \sigma_r|_{r=r_{cr}^-}. \tag{4.23}$$

The hoop stress in (3.7) and stiffness reduction factor in (3.12) at the critical crack boundary, which are utilised for calculating the radial stress, are given by

$$
\sigma_\theta|_{r=r_{\mathrm{cr}}^+} = \sigma_\theta|_{r=r_{\mathrm{cr}}^-} = \alpha f_t,
$$

$$
\beta|_{r=r_{\mathrm{cr}}^+} = \beta|_{r=r_{\mathrm{cr}}^-} = \frac{1}{1 + (n_c l_{\mathrm{ch}}/2\pi\alpha)(W_{\mathrm{cr}}/r_{\mathrm{cr}})}.
$$

(4.24)

And the radial strains in (3.11) at the critical crack boundary are given by

$$
\varepsilon_r|_{r=r_{\mathrm{cr}}^+} = \frac{f_t}{E}\left[\alpha + \frac{1-\alpha}{r_{\mathrm{cr}}(l_0^{\mathrm{cr}} - r_{\mathrm{cr}})\left[\delta(l_0^{\mathrm{cr}}, r_{\mathrm{cr}}) - \delta(l_0^{\mathrm{cr}}, r_y)\right]}\right],
$$

$$
\varepsilon_r|_{r=r_{\mathrm{cr}}^-} = \frac{f_t}{E}\left[\alpha + \frac{\alpha}{r_{\mathrm{cr}}(l_0^u - r_{\mathrm{cr}})\left[\delta(l_0^u, R_b) - \delta(l_0^u, r_{\mathrm{cr}})\right]}\frac{W_b - W_{\mathrm{cr}}}{W_u - W_{\mathrm{cr}}}\right].
$$

(4.25)

Consequently, (4.23) is expressed as

$$
(l_0^u - r_{\mathrm{cr}})\left[\delta(l_0^u, R_b) - \delta(l_0^u, r_{\mathrm{cr}})\right] - \frac{\alpha}{1-\alpha}\frac{W_b^u - W_{\mathrm{cr}}}{W_u - W_{\mathrm{cr}}}(l_0^{\mathrm{cr}} - r_{\mathrm{cr}})\left[\delta(l_0^{\mathrm{cr}}, r_{\mathrm{cr}}) - \delta(l_0^{\mathrm{cr}}, r_y)\right] = 0.
$$

(4.26)

The cracked front (r_y) and the critical crack front (r_{cr}) can be determined from the set of nonlinear equations, (4.22) and (4.26).

5. Completely Cracked Concrete Cover

After the crack front reaches the external surface, the concrete cover becomes completely cracked. Depending on the crack widths at the internal and external boundaries, three cases are considered, crack width within the concrete cover does not exceed the critical value ($W_b \leq W_{\mathrm{cr}}$ and $W_c \leq W_{\mathrm{cr}}$), critical crack propagates through the concrete cover ($W_b > W_{\mathrm{cr}}$ and $W_c < W_{\mathrm{cr}}$), and crack width within the concrete cover exceeds the critical value ($W_b > W_{\mathrm{cr}}$ and $W_c > W_{\mathrm{cr}}$).

5.1. Crack Width within Concrete Cover Not Exceeding Critical Value

A single cracked zone within the concrete cover exists in this case, and the crack width at the internal boundary does not exceed the critical value when the cover surface is cracked. To determine the two constant coefficients C_1 and C_2 in the general solution in (3.18), the unknown crack width at the external boundary W_c, together with the prescribed displacement at the internal boundary, is now utilised

$$
W|_{r=R_b} = W_b^{\mathrm{cr}}, \qquad W|_{r=R_c} = W_c.
$$

(5.1)

The normalised crack width over the concrete cover is then given by

$$W = \frac{\delta(l_0{}^{cr},r) - \delta(l_0{}^{cr},R_c)}{\delta(l_0{}^{cr},R_b) - \delta(l_0{}^{cr},R_c)} W_b{}^{cr} + \frac{\delta(l_0{}^{cr},R_b) - \delta(l_0{}^{cr},r)}{\delta(l_0{}^{cr},R_b) - \delta(l_0{}^{cr},R_c)} W_c. \tag{5.2}$$

To determine the unknown W_c, the free surface condition at the external boundary (R_c) described in (4.3) is adopted. The radial stress at the external boundary can be calculated from (3.13) by using the stiffness reduction factor in (3.12) and the first derivative of normalised crack width in (3.16), namely,

$$\beta|_{r=R_c} = \frac{1}{1 + (l_0{}^{cr}/R_c)((1-\alpha)W_c/W_{cr} - (1-\alpha)W_c)},$$

$$\left.\frac{dW}{dr}\right|_{r=R_c} = \frac{W_b{}^{cr} - W_c}{R_c(l_0{}^{cr} - R_c)^2 [\delta(l_0{}^{cr},R_b) - \delta(l_0{}^{cr},R_c)]}. \tag{5.3}$$

Then, the free surface condition at concrete cover surface gives

$$W_{cr} - (1-\alpha)W_c + \frac{(1-\alpha)(W_b{}^{cr} - W_c)}{R_c(l_0{}^{cr} - R_c)[\delta(l_0{}^{cr},R_b) - \delta(l_0{}^{cr},R_c)]}$$

$$+ \upsilon \sqrt{[W_{cr} - (1-\alpha)W_c] \cdot \left(W_{cr} - (1-\alpha)W_c + \frac{l_0{}^{cr}}{R_c}(1-\alpha)W_c\right)} = 0. \tag{5.4}$$

Once W_c is obtained, mechanical parameters of the completely cracked cover concrete, such as actual crack width, hoop residual strength and stiffness, and radial stress, can be calculated.

5.2. Critical Crack Propagation through Concrete Cover

The critical crack front divides the thick-walled cylinder into two zones: a cracked outer ring, where crack width does not exceed the critical value $(r_{cr}{}^+ \leq r \leq R_c)$, and a cracked inner ring, where crack width exceeds the critical value $(R_b \leq r \leq r_{cr}{}^-)$. For the cracked outer ring, two boundary conditions are considered: the critical crack width at the internal boundary $(r_{cr}{}^+)$ and the unknown crack width at the external boundary (R_c):

$$W|_{r=r_{cr}{}^+} = W_{cr}, \qquad W|_{r=R_c} = W_c. \tag{5.5}$$

The normalised crack width within the cracked outer ring is then expressed as

$$W = \frac{\delta(l_0{}^{cr},r) - \delta(l_0{}^{cr},R_c)}{\delta(l_0{}^{cr},r_{cr}) - \delta(l_0{}^{cr},R_c)} W_{cr} + \frac{\delta(l_0{}^{cr},r_{cr}) - \delta(l_0{}^{cr},r)}{\delta(l_0{}^{cr},r_{cr}) - \delta(l_0{}^{cr},R_c)} W_c. \tag{5.6}$$

For the cracked inner ring, the boundary conditions are

$$W|_{r=R_b} = W_b{}^u, \qquad W|_{r=r_{cr}{}^-} = W_{cr}. \tag{5.7}$$

The normalised crack width within the cracked inner ring is then given by

$$W = \frac{\delta(l_0{}^u, r) - \delta(l_0{}^u, r_{cr})}{\delta(l_0{}^u, R_b) - \delta(l_0{}^u, r_{cr})} W_b{}^u + \frac{\delta(l_0{}^u, R_b) - \delta(l_0{}^u, r)}{\delta(l_0{}^u, R_b) - \delta(l_0{}^u, r_{cr})} W_{cr}. \tag{5.8}$$

The free surface condition at the external boundary (R_c) of the cracked outer ring in this case gives an equation similar to (5.4) but involving unknown r_{cr}, namely,

$$W_{cr} - (1 - \alpha)W_c + \frac{(1 - \alpha)(W_{cr} - W_c)}{R_c(l_0{}^{cr} - R_c)[\delta(l_0{}^{cr}, r_{cr}) - \delta(l_0{}^{cr}, R_c)]}$$

$$\tag{5.9}$$

$$+ \upsilon \sqrt{[W_{cr} - (1 - \alpha)W_c] \cdot \left(W_{cr} - (1 - \alpha)W_c + \frac{l_0{}^{cr}}{R_c}(1 - \alpha)W_c\right)} = 0.$$

Meanwhile, the continuity condition of radial stresses at the critical boundary (r_{cr}) between the outer ring and the inner ring, described in (4.23), gives

$$\frac{W_{cr} - W_c}{W_{cr}}(l_0{}^u - r_{cr})[\delta(l_0{}^u, R_b) - \delta(l_0{}^u, r_{cr})]$$

$$\tag{5.10}$$

$$- \frac{\alpha}{1 - \alpha}\frac{W_b{}^u - W_{cr}}{W_u - W_{cr}}(l_0{}^{cr} - r_{cr})[\delta(l_0{}^{cr}, r_{cr}) - \delta(l_0{}^{cr}, R_c)] = 0.$$

Consequently, the two unknowns, W_c and r_{cr}, can be determined from the set of nonlinear equations, (5.9) and (5.10).

5.3. Crack Width Exceeding Critical Value within Concrete Cover

A single cracked zone is considered for the thick-walled cylinder in this case, and the crack width over the concrete cover now exceeds the critical value. The boundary conditions for this case are given by

$$W|_{r=R_b} = W_b{}^u, \qquad W|_{r=R_c} = W_c. \tag{5.11}$$

The normalised crack width within the cracked concrete cover is expressed as

$$W = \frac{\delta(l_0{}^u, r) - \delta(l_0{}^u, R_c)}{\delta(l_0{}^u, R_b) - \delta(l_0{}^u, R_c)} W_b{}^u + \frac{\delta(l_0{}^u, R_b) - \delta(l_0{}^u, r)}{\delta(l_0{}^u, R_b) - \delta(l_0{}^u, R_c)} W_c. \tag{5.12}$$

Similarly, from the free surface condition at the external surface (R_c), the unknown W_c can be determined from

$$(W_u - W_c) + \frac{1}{R_c(l_0{}^u - R_c)\left[\delta(l_0{}^u, R_b) - \delta(l_0{}^u, R_c)\right]}(W_b{}^u - W_c)$$
$$+ \upsilon\sqrt{(W_u - W_c)\left((W_u - W_c) + \frac{l_0{}^u}{R_c}W_c\right)} = 0. \tag{5.13}$$

When cracks in the cover concrete reach the ultimate cohesive width, the cracks become cohesionless and no residual strength exists in the cracked cover concrete. From (5.13), it can be seen that cracks at both the internal and external boundaries reach the ultimate cohesive width at the same time (T_u). The displacement at the internal boundary at time T_u is calculated from

$$\bar{u}_b(T_u) = \frac{\alpha W_u}{W_u - W_{cr}}\frac{f_t}{E}l_0{}^u. \tag{5.14}$$

The time at the end of cohesive cracking stage T_u can be then estimated by using (2.5) and (2.1).

6. Validation and Parameter Studies

6.1. Comparison of Theoretical Predictions with Experimental Data

To validate the proposed approach, the published experimental data such as the time to cracking on the concrete cover surface and the concrete crack width with reinforcement corrosion progress are adopted. Liu and Weyers [8] conducted experiments to measure the time to cracking induced by steel rebar corrosion for specimens with various corrosion rates and cover dimensions, as given in Table 1. The material properties for the specimens utilised in their study are taken as compressive strength f_c = 31.5 MPa, tensile strength f_t = 3.3 MPa, elastic modulus of concrete E = 27 GPa, Poisson's ratio υ = 0.18, concrete creep coefficient assumed here θ = 1, density of corrosion rust products ρ_r = 3600 kg/m^3, density of steel ρ_s = 7850 kg/m^3, and coefficient γ = 0.57. Other material properties adopted in the predictions are evaluated from the given concrete properties with assumed maximum aggregate size d_a = 25 mm, such as fracture energy G_f = 83 N/m, total crack number n_c = 4, critical crack width w_{cr} = 0.03 mm, and ultimate cohesive crack width w_u = 0.2 mm. The theoretical predictions of the time to cracking from the developed approach are then compared with the experimental data observed by Liu and Weyers [8], as shown in Table 1. As it can be seen from Table 1 the predicted results in general agree with the experimental results for various cover dimensions and corrosion rates. The discrepancy of the time to cracking for specimen S3 may be related to the fact that not all corrosion products are activated in the generation of radial pressure at the internal surface of the concrete cover. It should be noted that part of these products penetrates into the porous voids between the steel rebar and the surrounding concrete and a considerable amount of the rust transports into the surrounding cracks, in particular in the case when the corrosion rate is relatively higher, as discussed in the studies by Chernin et al. [14], Pantazopoulou and Papoulia [9], Liu and Weyers [8].

Table 1: Predicted and observed times to cracking on concrete cover surface.

Specimen number	Steel rebar diameter (mm)	Cover thickness (mm)	Corrosion rate ($\mu A/cm^2$)	Predicted time (year)	Observed time* (year)
S1	16	48	2.33	1.83	1.84
S2	16	70	1.79	3.44	3.54
S3	16	27	3.75	0.40	0.72
S4	12	52	1.80	2.20	2.38

*Experimental data from Liu and Weyers [8].
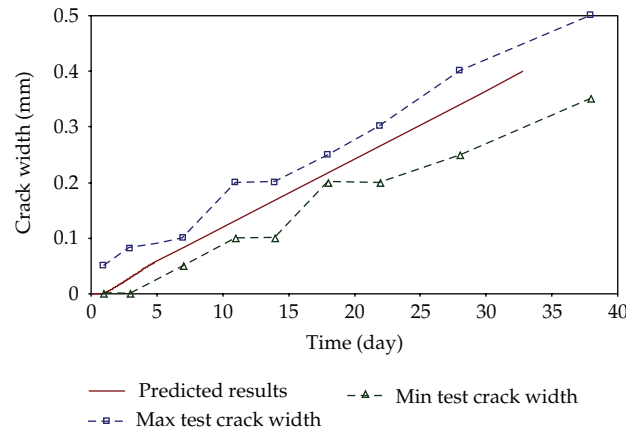
Figure 3: Comparison of predicted crack width over time with published experimental results.

The predicted results for the crack width on concrete cover surface with the progress of reinforcement corrosion are now compared with the experimental measurements presented by Andrade et al. [7], Molina et al. [22]. The experiments were carried out for steel rebar of 16 mm in diameter embedded into a concrete specimen with clear cover of 30 mm. The material properties utilised in their studies are taken as tensile strength f_t = 3.55 MPa, elastic modulus of concrete E = 36 GPa, and Poisson's ratio υ = 0.20. The decrease in diameter of the steel rebar due to corrosion over time is estimated from the corrosion rate i_{corr} = 100 $\mu A/cm^2$. Other material properties adopted in predictions include fracture energy G_f = 200 N/m, total crack number n_c = 4, critical crack width w_{cr} = 0.05 mm, and ultimate cohesive crack width w_u = 0.4 mm. The theoretical predictions of the crack width on the concrete cover surface over time are shown in Figure 3 to compare with the experimental measurements by Andrade et al. [7]. It can be seen that the predicted results lie between the maximum and minimum measured crack widths and are in good agreement with the experimental data.

6.2. Mechanical Parameter Studies

The specimen S1 shown in Table 1 and tested by Liu and Weyers [8] is now utilised to analyse the mechanical parameters with the reinforcement corrosion progress and through the concrete cover. The radial displacement $\overline{u}_b$ at the internal boundary of the concrete cover due to steel rebar corrosion is plotted with time in Figure 4. The expansive displacement at the rebar surface increases sharply at the early stage of corrosion and then grows steadily with
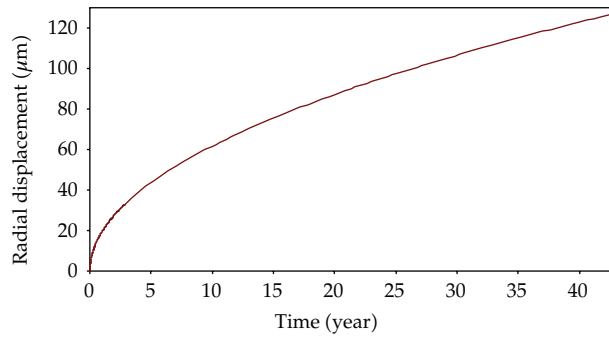
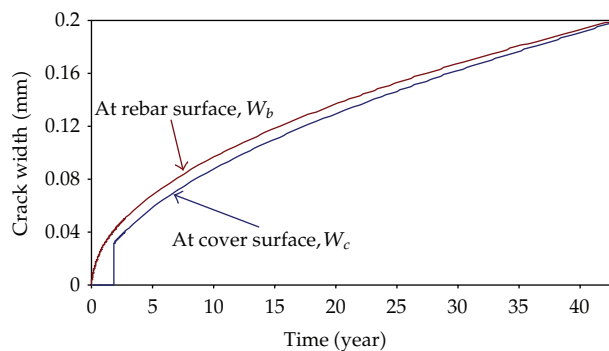**Figure 4:** Radial displacement at rebar surface with time t.

Figure 5: Crack widths at rebar surface (w_b) and at cover surface (w_c) with time t.

corrosion progress, reaching $127.3\,\mu$m when cracks get to ultimate cohesive width. Similar shape of curve is obtained for the crack width at the internal boundary of the concrete cover w_b, as shown in Figure 5. The crack width at the concrete cover surface w_c increases abruptly when crack front reaches the free cover surface due to sudden release of energy. After the time to cracking, the crack width at the cover surface w_c is close to that at the rebar surface w_b and becomes ultimate cohesive width at the time of 42.9 years.

   The plot in Figure 6 presents two sets of curves, the cracked front r_y and critical crack front r_{cr} propagating with time from the rebar surface to the concrete cover surface. The cracked front starts at the crack ignition time of 0.014 year when cracks appear at the internal boundary of the concrete cover and reaches the concrete cover surface at the predicted time to cracking of 1.83 years. Faster propagation of the cracked front is noted when the cracked front is near the internal boundary and the external boundary due to energy release. The critical crack front propagates gradually from the time of 0.97 year, but suddenly jumps to the concrete cover surface at the time to cracking.

   Figure 7 gives the history of hoop stresses σ_θ at the rebar surface and at the concrete cover surface with the progress of rebar corrosion. The hoop stress at the rebar surface quickly reaches tensile strength f_t at the crack ignition time of 0.014 year, followed by steady decrease to the time of 0.97 year when the crack width at the rebar surface becomes critical. From this point, the residual strength in the hoop direction at the rebar surface gradually reduces to zero at the time when cracks get to ultimate cohesive width. The residual strength at the cover surface experiences similar history to that at the rebar surface, but peaks at the time to
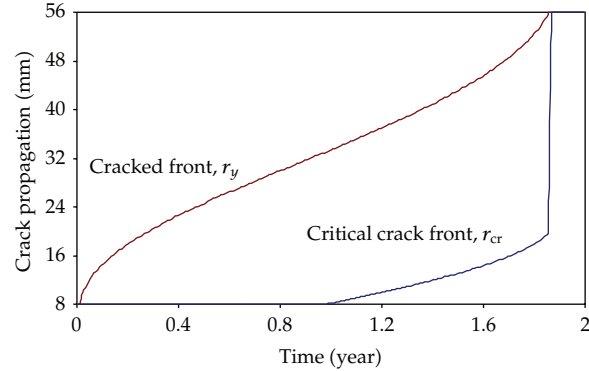
Figure 6: Propagation of cracked front (r_y) and critical crack front (r_{cr}) with time t.
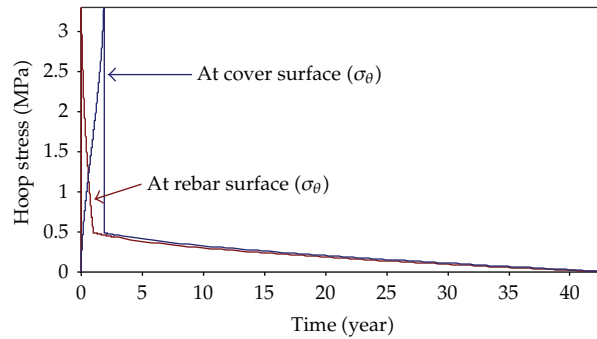

Figure 7: Hoop stress (σ_θ) at rebar surface and at cover surface with time t.

cracking followed by a sudden drop. The residual strengths at the rebar surface and at cover surface are very close to each other during the stage when the cover concrete is completely cracked. Figure 8 shows the histories of tangential stiffness reduction factor β at the rebar surface and at the concrete cover surface in logarithmic scale. Sharp changes are noted at the time of cracking initiation and at time when cracks become critical for the stiffness reduction factor at the rebar surface, and at the time to cracking for the stiffness reduction factor at the cover surface. It can be seen that the tangential residual stiffness decays faster than the tangential residual strength during the development of cracking in the cover concrete.

The bursting pressure σ_r exerted by the accumulating corrosion products at the internal boundary of the concrete cover is plotted in Figure 9. Radial pressure at the internal boundary builds up as cracks propagate from the rebar surface, reaching a peak value of 15.2 MPa (well below concrete compressive strength of 31.5 MPa) at the time of 1.21 years when crack front travelled about 2/3 of the concrete cover. Sudden release of the radial pressure occurs at the time when crack front reaches the cover surface, and residual radial pressure maintains only about 1/4 of the peak value after the time to cracking. The sudden release of radial pressure indicates significant reduction of the bond strength between the steel rebar and the surrounding concrete cover after the time to cracking.

Figures 10–13 present results of crack width w, hoop stress σ_θ, hoop stiffness reduction factor β, and radial stress σ_r varying with the radius within the concrete cover. Six important times during concrete cracking evolution are selected and listed in Table 2. The results in
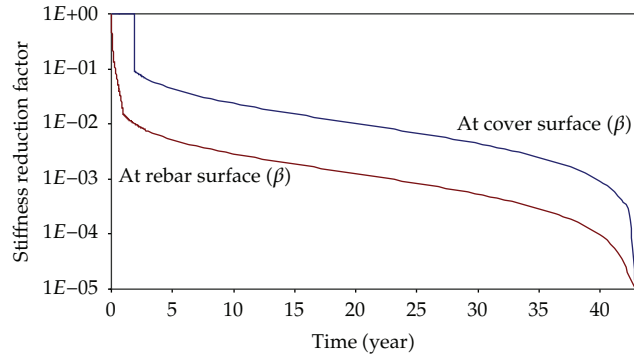
Figure 8: Hoop stiffness reduction factor (β) at rebar surface and at cover surface with time t.
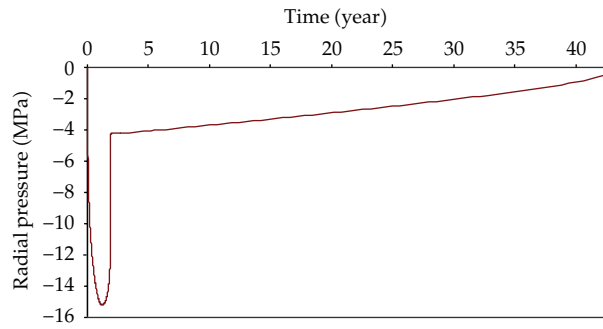

Figure 9: Radial pressure (σ_r) at rebar surface with time t.
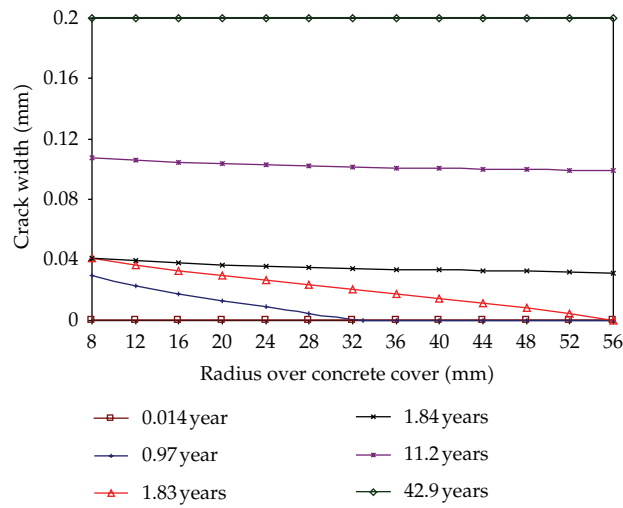

Figure 10: Crack width (w) varying over concrete cover at various times.
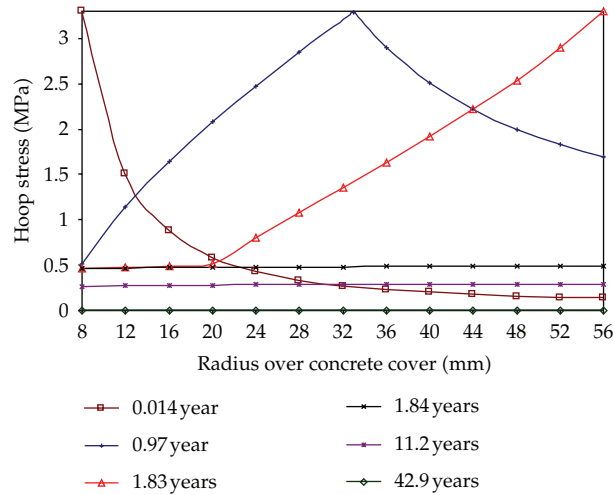
Figure 11: Hoop stress (σ_θ) varying over concrete cover at various times.
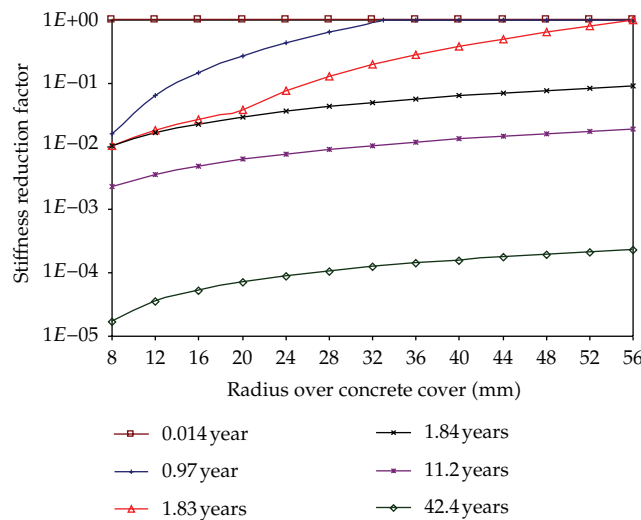

Figure 12: Stiffness reduction factor (β) varying over concrete cover at various times.

Figure 10 show that the crack widths over the concrete cover indicate cracks open approximately in a wedge shape before the time to cracking. The crack width has no significant change over the concrete cover thereafter and eventually gets to the ultimate cohesive width through the concrete cover. As shown in Figure 11, the peak values of hoop stress indicate the cracked front propagation through the concrete cover before the time to cracking. The residual strength in hoop direction has little change over the concrete cover after the time to cracking, becoming zero at the time when the cracks reach the ultimate cohesive width. The results plotted in Figure 12 show that the hoop stiffness reduction factors change significantly at the cracked fronts during crack propagation through the concrete cover and reduce sharply after concrete is cracked. The radial stresses shown in Figure 13 have peak values at the internal boundary of the concrete cover, decreasing fast with the increase of radius within
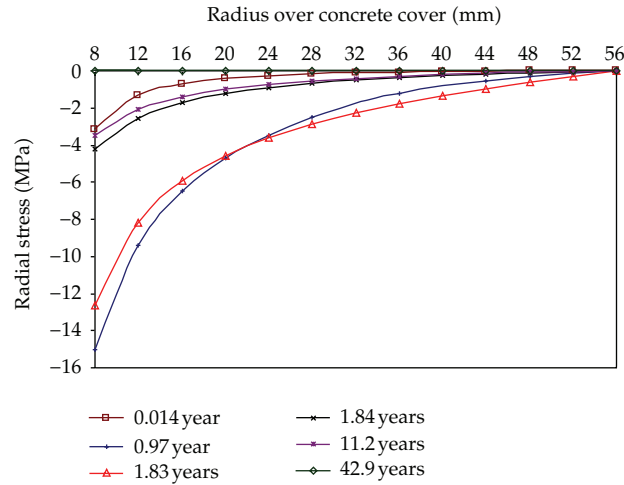
Figure 13: Radial stress (σ_r) varying over concrete cover at various times.

Table 2: Selected times during cover concrete cracking evolution.

Time	Concrete crack evaluation
0.014 year	Cracking initiation at internal boundary
0.97 year	Critical cracks developed at internal boundary
1.83 years	Cracks reaching at external surface
1.84 years	Cracks just occurred at external surface
11.2 years	Cracks reaching 1/2 ultimate cohesive width at external boundary
42.9 years	Cracks reaching ultimate cohesive width over concrete cover

the concrete cover to a value of zero at the free surface boundary. The radial stresses drop to only approximately 1/5 of the peak value at the middle of concrete cover.

7. Conclusions

A new method for theoretically analysing the evolution of cracking in concrete cover subject to expansive internal displacement caused by steel rebar corrosion is presented based on the thick-walled cylinder model for the concrete cover and the tensile softening model for the cracked concrete. The governing equation for directly solving the crack width in the cracked concrete is established and a general closed-form solution is obtained for the proposed boundary value problem. The formulas for calculating actual crack width as well as other mechanical parameters of the cracked concrete, including residual strength, residual stiffness, and radial stress, are derived for various stages during the cracking evolution in the cover concrete. The predicted results for the time to cracking for various concrete cover dimensions and reinforcement corrosion rates and for the crack width over time are examined and demonstrated to be in good agreement with the published experimental measurements.

The time taken for cracked front to propagate from the internal boundary of the concrete cover to the cover surface is substantially long, and the existing models for estimating the time to cracking on the cover surface by ignoring the crack propagation through the concrete cover may be improper. The time to cracking is a function of cover

dimensions, concrete material properties, and reinforcement corrosion rate. The crack width of the concrete cover depends on concrete material properties and the expansive displacement developed at the internal boundary due to reinforcement corrosion. The residual stiffness in hoop direction reduces significantly when concrete is cracked and decays faster than the hoop residual strength. The radial pressure at the interface between the steel rebar and the concrete cover reaches peak value well before the cracks occur at the cover surface, drops suddenly when concrete becomes completely cracked through the cover, and decays fast from the bond interface over the concrete cover. The time taken for cracks to reach the ultimate cohesive width and for hoop residual strength and stiffness to vanish is relatively long, comparing with the time to cracking.

References

[1] Z. P. Bazant, "Physical model for steel corrosion in concrete sea structures—theory," *Journal of the Structural Division*, vol. 105, no. 6, pp. 1137–1153, 1979.

[2] D. Meyer, "A statistical comparison of accelerated concrete testing methods," *Journal of Applied Mathematics and Decision Sciences*, vol. 1, no. 2, pp. 89–100, 1997.

[3] A. A. Torres-Acosta and M. Martinez-Madrid, "Residual life of corroding reinforced concrete structures in marine environment," *Journal of Materials in Civil Engineering*, vol. 15, no. 4, pp. 344–353, 2003.

[4] M. A. Torres and S. E. Ruiz, "Structural reliability evaluation considering capacity degradation over time," *Engineering Structures*, vol. 29, no. 9, pp. 2183–2192, 2007.

[5] T. Vidal, A. Castel, and R. Francois, "Analyzing crack width to predict corrosion in reinforced concrete," *Cement and Concrete Research*, vol. 34, no. 1, pp. 165–174, 2004.

[6] G. J. Al-Sulaimani, M. Kaleemullah, I. A. Basunbul, and Rasheeduzzafar, "Influence of corrosion and cracking on bond behaviour and strength of reinforced concrete members," *ACI Structural Journal*, vol. 87, no. 2, pp. 220–231, 1990.

[7] C. Andrade, C. Alonso, and F. J. Molina, "Cover cracking as a function of bar corrosion: part I—experimental test," *Materials and Structures*, vol. 26, no. 8, pp. 453–464, 1993.

[8] Y. Liu and R. E. Weyers, "Modelling the time-to-corrosion cracking in chloride contaminated reinforced concrete structures," *ACI Materials Journal*, vol. 95, no. 6, pp. 675–681, 1998.

[9] S. J. Pantazopoulou and K. D. Papoulia, "Modelling cover cracking due to reinforcement corrosion in RC structures," *Journal of Engineering Mechanics*, vol. 127, no. 4, pp. 342–351, 2001.

[10] D. Coronelli, "Corrosion cracking and bond strength modeling for corroded bars in reinforced concrete," *ACI Structural Journal*, vol. 99, no. 3, pp. 267–276, 2002.

[11] K. Bhargava, A. K. Ghosh, Y. Mori, and S. Ramanujam, "Model for cover cracking due to rebar corrosion in RC structures," *Engineering Structures*, vol. 28, no. 8, pp. 1093–1109, 2006.

[12] R. Tepfers, "Cracking of concrete cover along anchored deformed reinforcing bars," *Magazine of Concrete Research*, vol. 31, no. 106, pp. 3–12, 1979.

[13] B. S. Jang and B. H. Oh, "Effects of non-uniform corrosion on the cracking and service life of reinforced concrete structures," *Cement and Concrete Research*, vol. 40, no. 9, pp. 1441–1450, 2010.

[14] L. Chernin, D. V. Val, and K. Y. Volokh, "Analytical modelling of concrete cover cracking caused by corrosion of reinforcement," *Materials and Structures*, vol. 43, no. 4, pp. 543–556, 2010.

[15] Z. P. Bažant and J. Planas, *Fracture and Size Effect in Concrete and Other Quasibrittle Materials*, CRC Press, Boca Raton, Fla USA, 1998.

[16] Z. P. Bažant and A. Zubelewicz, "Strain-softening bar and beam: exact non-local solution," *International Journal of Solids and Structures*, vol. 24, no. 7, pp. 659–673, 1988.

[17] A. Hillerborg, M. Modéer, and P. E. Petersson, "Analysis of crack formation and crack growth in concrete by means of fracture mechanics and finite elements," *Cement and Concrete Research*, vol. 6, no. 6, pp. 773–782, 1976.

[18] Comité Euro-International du Béton-Fédération International de la Pré-contrainte (CEB-FIP), *Design Code*, Thomas Telford, London, UK, 1990.

[19] Z. P. Bažant and B. H. Oh, "Crack band theory for fracture of concrete," *Materials and Structures*, vol. 16, no. 3, pp. 155–177, 1983.

[20] C. V. Nielsen and N. Bićanić, "Radial fictitious cracking of thick-walled cylinder due to bar pull-out," *Magazine of Concrete Research*, vol. 54, no. 3, pp. 215–221, 2002.

[21] S. P. Timoshenko and J. N. Goodier, *Theory of Elasticity*, McGraw-Hill, New York, NY, USA, 3rd edition, 1970.

[22] F. J. Molina, C. Alonso, and C. Andrade, "Cover cracking as a function of rebar corrosion: part 2—numerical model," *Materials and Structures*, vol. 26, no. 9, pp. 532–548, 1993.